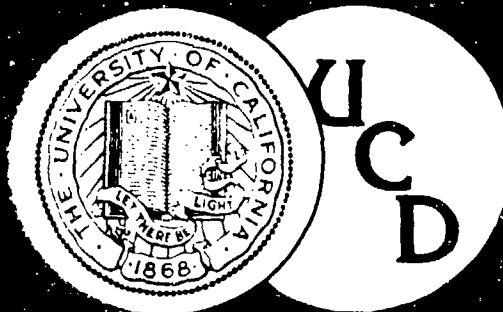


AD-A149 666

## University of California, Davis



THIS IS A COPY

ANALYSIS AND COMPUTATIONS OF  
MICROWAVE-ATMOSPHERIC INTERACTIONSWee Woo, Senior Investigator  
and J. S. DeGroot, Principal InvestigatorFinal Report for the Period September 1, 1982  
to August 31, 1983

NAVAIR N00019-82-C-0448

PRG R-98

June 1, 1984

DTIC  
ELECTRONIC

DEC 21 1984

A

APPROVED FOR PUBLIC RELEASE:  
DISTRIBUTION UNLIMITEDDepartment of Applied Science  
Plasma Research Group

# TABLE OF CONTENTS

I. Introduction	1.
II. Summary of Previous Results	3.
III. Simulations of NRL Microwave Experiments	9.
IV. Collective Plasma Effects due to Microwaves	14.
V. Summary	16.
VI. Acknowledgements	18.
VII. References	19.
VIII. Figure 1	20.
IX. Figure 2	21.
X. Figure 3	22.
XI. Figure 4	23.
XII. Figure 5	24.



TITLE: AUTH: DATE: ORGANIZATION: DISTRIBUTION:	
Distribution/	
Availability Codes	
Dist A-1	Avail and/or Special

APPROVED FOR PUBLIC RELEASE  
DISTRIBUTION UNLIMITED

## I. Introduction

The Plasma Research Group of the University of California at Davis has continued the theoretical investigation of microwave - atmospheric interactions, in close coordination with personnel at the Naval Research Laboratory and elsewhere. This report covers the period September 1, 1982 to August 31, 1983.

We have made advances in the following areas: (1) Continuation of the previous survey to gain more insight into the important phenomena; (2) detailed comparison of the recent NRL focused microwave experiments with our theory; (3) discussion of important collective plasma effects.

The basic investigation concerns the propagation and absorption of microwaves above the breakdown threshold in the atmosphere with the self-consistent breakdown plasma. Typical hydrodynamic calculations show that an ionization front is rapidly formed which moves toward the microwave source and consequently decouples the microwaves from the original ionization region. By focusing the microwaves or using a reflector, ionization can be confined to localized regions where the microwave strength is high enough to cause breakdown even though the incoming microwaves are below threshold. In a strongly

collisional atmosphere, it is found that the cutoff plasma density, which roughly equals the collisionless cutoff density multiplied by the collisionality, is much higher than the calculated maximum density. This results in high absorption that increases with microwave power, decreases with atmospheric pressure, and is quite independent of other parameters. In a weakly collisional atmosphere, breakdown easily creates a plasma density higher than the cutoff density and causes reflection. It is found that the reflection decreases with the collisionality of the system and is quite independent of the microwave strength. In general, the microwave field strength in the ionization regions is attenuated to the breakdown value at steady state, and the resulting electron temperature is about 2 eV, independent of the incident microwave flux. Limitations of the calculations are due to the availability of experimental data for the rate coefficients, but comparison to results from recent focused microwave experiments shows excellent agreement.

In addition, collective plasma effects, such as parametric instabilities, resonant absorption and the ponderomotive force due to the microwaves are also investigated.

## II. SUMMARY OF PREVIOUS RESULTS

The previous investigation concerns mainly the build-up of plasma due to the breakdown, or the ionization of air, which strongly affects the propagation of the microwaves. In the past, most studies and measurements were done<sup>1</sup> near the breakdown thresholds. Recently experiments have been performed<sup>2</sup> for microwave power higher than the threshold, to study the behavior of the plasma after breakdown.

If we neglect free electron diffusion, experimental data show that the breakdown threshold is roughly given by  $E_{rms} \sim 32 \sqrt{p_{Torr}^2 + 2 f_{GHz}^2}$ , here  $E_{rms}$  is the rms electric field in volt/cm,  $p$  is the atmospheric pressure and  $f$  is the microwave frequency (the subscripts indicate the units). At sea level ( $p_{Torr} \gg f_{GHz}$ ), the microwave power flux breakdown threshold is about  $1.5 \text{ MW/cm}^2$ . This kind of power is achievable using present technology. Free electron diffusion is only important in weakly collisional air and at the time of breakdown, and can be ignored once the plasma builds up; this is the stage we are most interested in.

After breakdown, the plasma density grows exponentially in time quickly until the density is high enough for reflection and absorption of the microwaves. The microwave-plasma

interaction is basically dominated by electron-neutral collisions in which the collision frequency is roughly given by  $\nu_c \sim 5 \times 10^9 P_{\text{Torr}}$  at sufficiently high microwave power. In the important frequency range of a few GHz to several hundred GHz the system is very collisional in the lower atmosphere ( $\nu_c/\omega \gg 1$ , where  $\omega = 2\pi f$  is the angular frequency of the microwaves). In this case the cut-off plasma density of the microwaves is given by  $n/n_c \sim \nu_c/\omega$ , here  $n_c = 1.26 \times 10^{-8} f^2 \text{ cm}^{-3}$  is the critical density, instead of the usual  $n \sim n_c$  in the collisionless case.

We had shown that reflection depends mainly upon the height and the slope of the density profile. In the strongly collisional limit, reflection becomes important when  $k_0 \ell < 1$  and  $n/n_c > \nu_c/\omega$ , here  $k_0$  is the wavenumber of the microwaves and  $\ell$  is the scale length of the density gradient. In the weak collisional limit, they are given by  $k_0 \ell < \omega/\nu_c$  and  $n/n_c > 1$ . In useful atmospheric units, the conditions for the two limits are given by  $\ell(\text{cm}) < f_{\text{GHz}}^{-1}$  and  $n(\text{cm}^{-3}) > 10^{13} P_{\text{atm}} f_{\text{GHz}}$  valid for  $P_{\text{atm}} > 10^{-3} f_{\text{GHz}}$ , and  $\ell(\text{cm}) < 10^{-2} P_{\text{atm}}$  and  $n(\text{cm}^{-3}) > 10^{10} f_{\text{GHz}}^2$  valid for  $P_{\text{atm}} < 10^{-3} f_{\text{GHz}}$  respectively.

In very collisional air, the condition for good absorption is given by  $(n/n_c)(k \Delta) > \nu_c/\omega$ , here  $\Delta$  is the width of

tion is given by  $(n/n_c)(k\Delta) \nu_c/\omega$ , here  $\Delta$  is the width of the density profile. Rewritten into atmospheric units, this is  $n\Delta(\text{cm}^{-2}) > 10^{13} P_{\text{atm}}$  or  $(n/N)\Delta(\text{cm}) > 10^{-6}$ , here  $N$  is the atmospheric density. Therefore only low ionization of the air is needed to give good absorption.

The currently available experimental data were mainly obtained in dc experiments and are roughly valid in the range  $0 < E_{\text{rms}}/P_{\text{Torr}} < 100$  within an accuracy of 10 to 20%. Checking the relation of the data to the kinetic description carefully, we can relate<sup>1</sup> the data to an effective microwave field strength which is defined by  $E(1 + \omega^2/\nu_c^2)^{-1/2}$ . Therefore the rate coefficients (which are elastic collision, ionization, and attachment) and thermal energy of the electrons, can be determined macroscopically as functions of microwave field strength without knowing the details of the microscopic kinetic description.

We present hydrodynamic calculations for both planar and spherical geometries. A problem that must be avoided is the growth of the plasma density in all space. After some time the density even grows faster at places close to the microwave source because the field strength is stronger there due to reflection. Eventually the microwaves will be cut-off by a very high plasma density near the source.

In the planar case, we present two types of calculations. First, a local region is pre-ionized by other means, then the pre-ionized plasma grows to high enough density to cause high absorption before the density at other places grows significantly. During this time, a steady state ionization front is formed and moves rapidly toward the microwave source.

Second, a reflector is placed at a boundary, such that standing microwaves are formed in the system. The incoming power is below the breakdown threshold, therefore the problem of cutting-off the microwaves near the source can be avoided. However the maxima of the standing wave can be above the threshold, and the multi-peak plasma density is formed and the microwaves are absorbed. Stationary state absorption is obtained in this case.

In very collisional air, results for both cases show that the product  $n \Delta$  (sum for multi-peak density) of the asymptotic plasma density profile remains roughly the same at fixed microwave power and atmospheric pressure, and is quite independent of other parameters. Therefore it gives fixed absorption. The reason is that the microwaves have to be attenuated to the breakdown value  $E_{rms} \sim 32 p_{Torr}$  in the density profile in order that a steady state is achieved. Thus the required attenuation fixes the product of  $n$  and therefore the absorp-



absorption. Energy that is not absorbed will be transmitted in the pre-ionization case because the density required for significant reflection is not built up.

We also find that the asymptotic absorption increases rapidly with the microwave power and inversely with pressure. Total absorption occurs for power not very much higher than the threshold.

In weakly collisional air, the reflection density is easier to be built up. We also find that the reflection decreases with  $\nu_c/\omega$ , the collisionality of the system, and is quite independent of the microwave strength. The energy that is not reflected will be absorbed due to the longer elongated density profile at the back in the pre-ionization case.

In spherical geometry, which simulates converging microwaves, the cut-off problem is also avoided because the microwave beams are above breakdown threshold only near the focal region. We find that one after another density peaks are created at the end close to the focus, and they move toward the microwave source. However the density peaks cannot move beyond a certain point in the system because the field strength is below the threshold beyond it. Asymptotic absorption is also obtained in this geometry, however, it increases

with system length and beam convergence.

In all planar and spherical calculations, the electron temperature tends to be roughly 2 eV in steady state since the microwave strength is roughly the breakdown strength.

We have also simulated the recent focused microwave experiments<sup>2</sup> by two connected regions with different spherical convergence with and without a reflector at the focus. The ionization occurs initially near the focus, however the plasma grows much denser near the threshold region at later time and decouples the microwaves from the focal region. The length, location and motion of the plasma density profiles are in excellent agreement with those of the experiments.

## III. SIMULATIONS OF NRL MICROWAVE EXPERIMENTS

We have compared the NRL experiments, (Figure 1) with our calculations previously. The experimental and theoretical results are described in the following. In the experiments<sup>2</sup> carried out at NRL the microwaves (frequency 35 GHz and Power 112 kW) are focused through a lens (7.6 cm diameter and 11.2 cm focal length) into the nitrogen gas (25 Torr). The measured elliptic area of the focus is  $\pi \times 0.55 \text{ cm} \times 0.75 \text{ cm}$ . Using a circular area to model the measured elliptic area, the equivalent radius is 0.64 cm. The radial profile of the microwaves is approximated by a Gaussian with an e-folding distance of 0.77 cm. The maximum power flux is 60 kW/cm<sup>2</sup> (equivalent to the total power evenly distributed in a circle of radius 0.77 cm) at the axis.

The diffraction of the microwaves starts to occur at an axial distance of 3.5 cm (4 wavelengths) from the focus. Between this point and the lens, the microwaves are focused spherically. Our simulation starts at an axial distance of about 6 cm (7 wavelengths) from the focus with  $I \approx 8.2 \text{ kW/cm}^2$  at the axis (equivalent to the total power evenly distributed in a circle of radius 2.1 cm). The microwaves are focused spherically in a distance of 2.5 cm and connected to the solution in the diffraction region (3.5  $\rightarrow$  0 cm). We ap-

proximate the diffraction effect by another spherical effect of aspect ratio 1.55 (equivalent to a 0.77 cm radius circle at focus and 1.2 cm radius circle at 3.5 cm). The schematic of the simulation region is shown in Figure 1.

Although the coefficients in our computer code are for air, the code can be used to approximate  $N_2$  gas. As in the experiments, two cases are run with and without a metallic reflector placed at the focus. The microwave pulse length is 1  $\mu$ sec.

In the case without reflector, the spatial profiles are presented in Figures 2 and 3 (microwaves incoming from the left). At  $t = 50$  nsec, the ionization of the air by the microwaves occurs mainly near the focus (Figure 2 a), however, at the same time the microwaves are attenuated there due to the presence of the plasma (Figure 3 a). The associated electron temperature is plotted in Figure 3 (b).

At  $t = 100$  nsec, the plasma grows faster near the connection region (Figure 2 b) because the microwaves are stronger there. At  $t = 400$  nsec, the plasma at the ionization front reaches the collisionless critical density and becomes thicker (Figure 2 c), thus the microwaves are decoupled from the focal region. The ionization front moves slowly toward the mi-

crowave source until at  $t = 1 \mu\text{sec}$  (Figure 2 d), and the front cannot move beyond 6 cm because the microwave strength is below the breakdown threshold beyond that point. The decoupling of the microwaves from the focal region at  $1 \mu\text{sec}$  is shown in Figure 3 (a).

The calculated profiles agree quite well with those from the experiments without a reflector (the frame pictures presented in Figure 2 of reference 2). The common observations are (1) the initial less dense plasma near the focal region, (2) the much denser plasma just inside the breakdown region at later times, (3) the slow motion of the denser plasma at later times, and (4) the length of the ionization region being about 5 cm.

Our calculated plasma density ( $4 \times 10^{12} - 2 \times 10^{13} \text{ cm}^{-3}$ ) is also within the experimental measured range. Also, our calculated electron temperature is roughly an eV lower. The higher experimental value is probably due to the use of 15 Torr  $\text{N}_2$  and 19 Torr He at the time of the measurement of the electron temperature. Another explanation for the measurements is due to the two dimensional effects.

The calculated spatial profiles are presented in Figures 4 and 5 for the case of a metal reflector at the focus perpen-

dicular to the incoming microwaves. Because of the standing waves set up by the reflector, the initial ionization is stronger and spatially more non-uniform than in the previous case. This is shown in Figure 4 (a) for an early time,  $t = 10$  nsec. The standing wave characteristic is shown in Figure 5 (a) with the microwaves attenuated near the focus due to the presence of the plasma.

As in previous cases, the plasma grows faster near the connection region and moves out slowly as shown in Figures 4 (b), (c), and (d) at  $t = 100$ , 400 and 1000 nsec respectively. However, the denser plasma profile in this case is split due to the growth of the spikes. The decoupling of the microwaves from the focal region at  $t = 1 \mu\text{sec}$  is shown in Figure 5 (b).

Qualitatively the cases without and with reflector are similar. This is consistent with the observations in the experiment (Figures 2 and 3 in Reference 2 for the two cases). The additional features due to the presence of the reflector shown in the frame pictures are (1) stronger ionization in the focal region at early time and (2) the spiky feature. In general, similar results are obtained at later times due to the strong absorption ( $A \geq 90\%$ ) of the microwaves by the plasma, such that reflection by the reflector is not important.

The motion of the ionization front and the decoupling of the microwaves can be seen in the time plots as shown in above figures. As quickly as 50 nsec, the microwaves are decoupled from the focal region. After that the ionization front moves slowly just inside the breakdown region. The speed of the ionization front is obviously a function of time. The average speed is 4 to 5 x 10<sup>6</sup> cm/sec. The time plots agrees with the experimental observations (Figure 3 b in Reference 2).

The one dimensional calculations compare well with the experimental results. Some possible two dimensional effects should be investigated further. However the breakdown should not be strongly affected by the two dimensional effects because these are low pressure experiments.

#### IV. COLLECTIVE PLASMA EFFECTS DUE TO MICROWAVES

In addition to the microwave absorption mentioned above, which is due to electron-neutral collisions, if the microwave field is high enough, the plasma is unstable to the growth of parametric instabilities<sup>3</sup>. The threshold of the parametric decay instability can be estimated by using the electron-neutral and ion-neutral collision frequencies, which is given by  $I \sim 4.2 \times 10^{13} \times P_{\text{atm}}^4 u_e (1 + 2.8 \times 10^{-6} f_{\text{GHz}}^2 / P_{\text{atm}}^2) / f_{\text{GHz}}^2$ , here  $u_e$  is the electron thermal energy in eV and  $I$  is microwave power flu in  $\text{Watt/cm}^2$ . For  $f_{\text{GHz}} = 3$ ,  $P_{\text{atm}} = 10^{-2}$  (an altitude 30 km), and  $u_e = 2$  eV,  $I \sim 10^5 \text{ W/cm}^2$ . Therefore the parametric instabilities are important at high altitudes (varies as  $p^4$ ) and high frequencies. Microwaves are absorbed and the energy is deposited in the hot tail of electron distribution.

An alternative way to increase the microwave absorption is to use p-polarized microwaves. The p-polarized microwaves, with one of the electric field components along the plasma density gradient, could drive electrostatic waves in the same direction. Electrons are slowly heated by the excited electrostatic waves resulting in resonant absorption of the microwaves. The absorption<sup>4</sup> can be as high as 50%.

Propagation of microwaves is possible even after break-



down. The point is that the ponderomotive force<sup>5</sup> (the radiation pressure) of the microwaves can be large enough to expel plasma from the breakdown region. After the plasma density is low enough, the microwaves can tunnel through the breakdown channel. This effect is more important at high altitudes and high frequencies. The ponderomotive force is inversely proportional to the square of the electron collision frequency so it increases rapidly with altitude. Effects due to the ponderomotive force become important at a power of roughly  $10^5 \text{ W/cm}^2$  at an altitude of 30 km (roughly 100 times the CW breakdown threshold). Thus, channel formation is possible at this power flux.

## V. SUMMARY

We have investigated the air breakdown due to microwaves propagating in the atmosphere. The important processes are electron-neutral collisions, ionization, attachment, and excitation. Thermal equilibrium of the electrons with the microwaves is also obtained from available experimental data. Some previous results are summarized as follows.

Reflection and absorption of the microwaves in the presence of the plasma density profiles are investigated both analytically and numerically. Conditions for reflection and absorption are obtained.

Hydrodynamic calculations in planar geometry were carried out for two cases: pre-ionization in a localized region initially and with a reflector at a boundary. In the first case, enough microwave energy can be absorbed in the time interval of interest, whereas a stationary state can be achieved in the second case. Calculations in spherical geometry show that many density peaks emerge from the end close to the focus and decelerate toward the microwave source.

Some typical planar results show that the air is ionized rapidly to form an ionization front moving toward the mi-

crowave source which consequently decouples the microwaves from the original region. By focusing the microwaves or using a reflector, localized regions can be heated by the microwaves.

The electron temperature obtained tends to be roughly 2 eV at steady state regardless of the microwave power. The heated electrons are able to exchange energy with the neutral atmospheric molecules<sup>5</sup> and will enhance the neutral temperature.

At high altitude, the heating of electrons by other mechanisms, such as the collective plasma effects, is possible. Two effects, parametric instabilities<sup>3</sup> and resonant absorption<sup>4</sup>, can result in heating suprathermal electrons to higher temperature.

The limitations of the calculations are due to the availability of the experimental data for the rate coefficients. Nevertheless, comparison of the calculations with recent microwave experiments<sup>2</sup> give excellent agreement.

# ACKNOWLEDGMENTS

This work was supported by Naval Air Systems Command  
under Contract N00019-82-C-0448.

# REFERENCES

1. A. D. MacDonald, D. U. Gaskell, and H. N. Gitterman, Phys. Rev. 5, 1841, (1963), and references therein.
2. W. M. Bollen, C. L. Yee, A. W. Ali, M. J. Nagurney, and M. E. Reed, J. Appl. Phys. 54, 101, (1983).
3. K. Mizuno and J.S. DeGroot, Phys. Rev. Lett.35, 219 (1975); P.W. Rambo, Wee Woo, J.S. DeGroot, and K. Mizuno, to be published in Phys. Fluids,(1984)
4. K. Mizuno, J.S. DeGroot, and F. Kehl, Phys. Rev. Lett. 49, 1004 (1982)
5. S.C. Lin and G.P. Theofilos, Phys. Fluids 6, 1369 (1963)

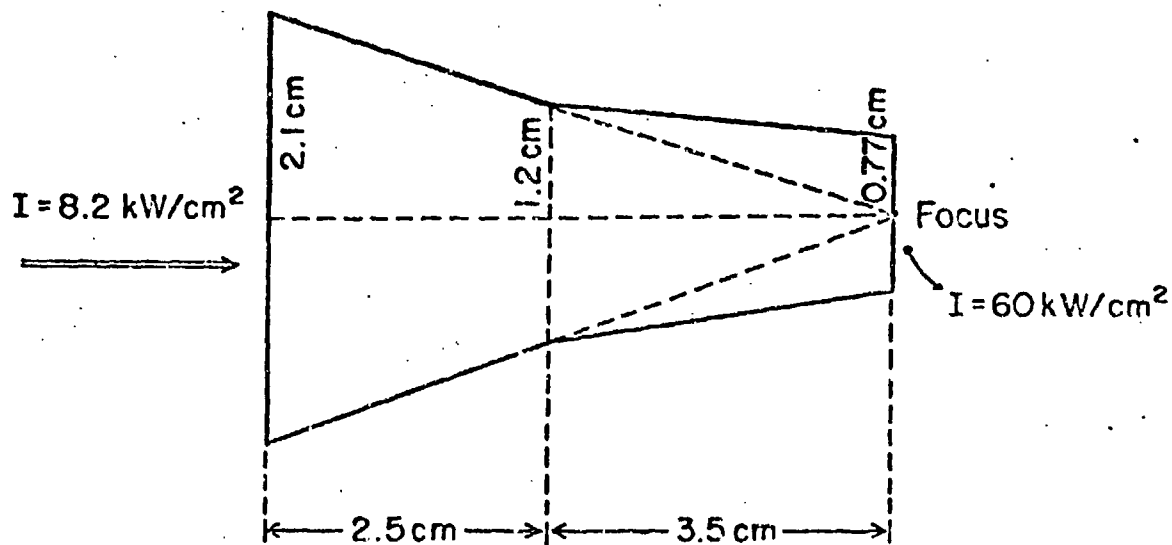


FIGURE 1

Schematic of the geometry for calculations to simulate the focused microwave experiments with  $p = 25 \text{ Torr}$ ,  $f = 35 \text{ GHz}$  and power 112 kW. The estimated power fluxes on the axis are shown and diffraction (simulated by another spherical effect) starts roughly 3.5 cm from the focus.

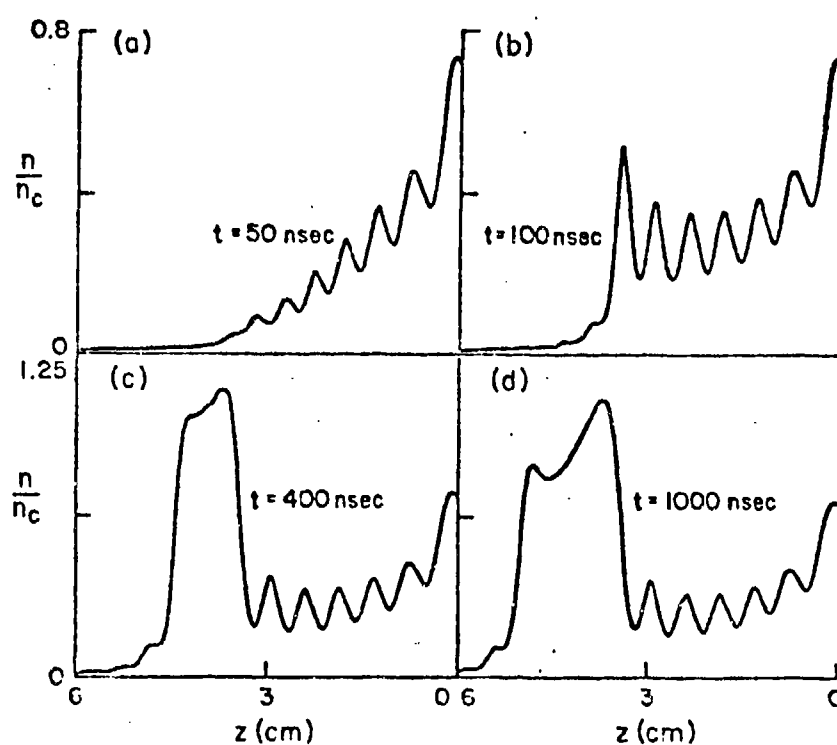


FIGURE 2

Density profiles at 4 different times for the case without reflector. The ionization occurs initially near the focus, however, the focal region is decoupled from the microwaves due to the stronger ionization near the connection region at later times.

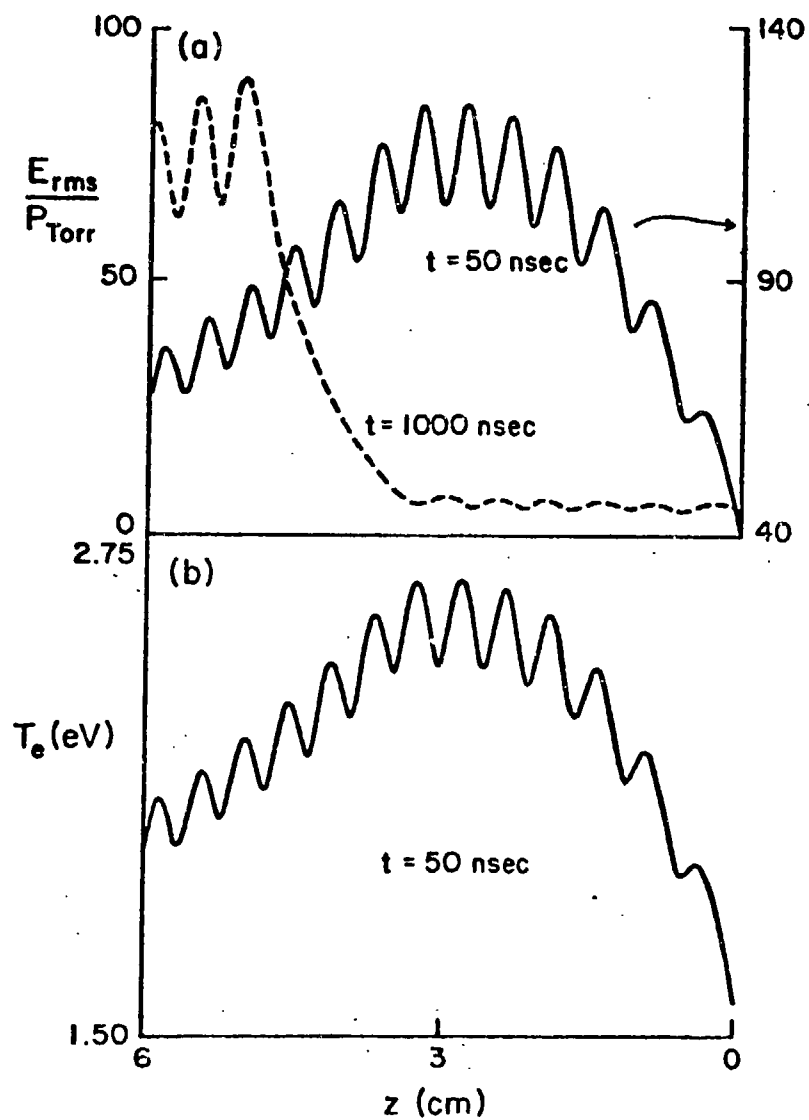


FIGURE 3

Microwave and temperature profiles corresponding to the plots shown in Figure 2. Microwaves are decoupled from the focal region as shown at  $t = 1000$  nsec.



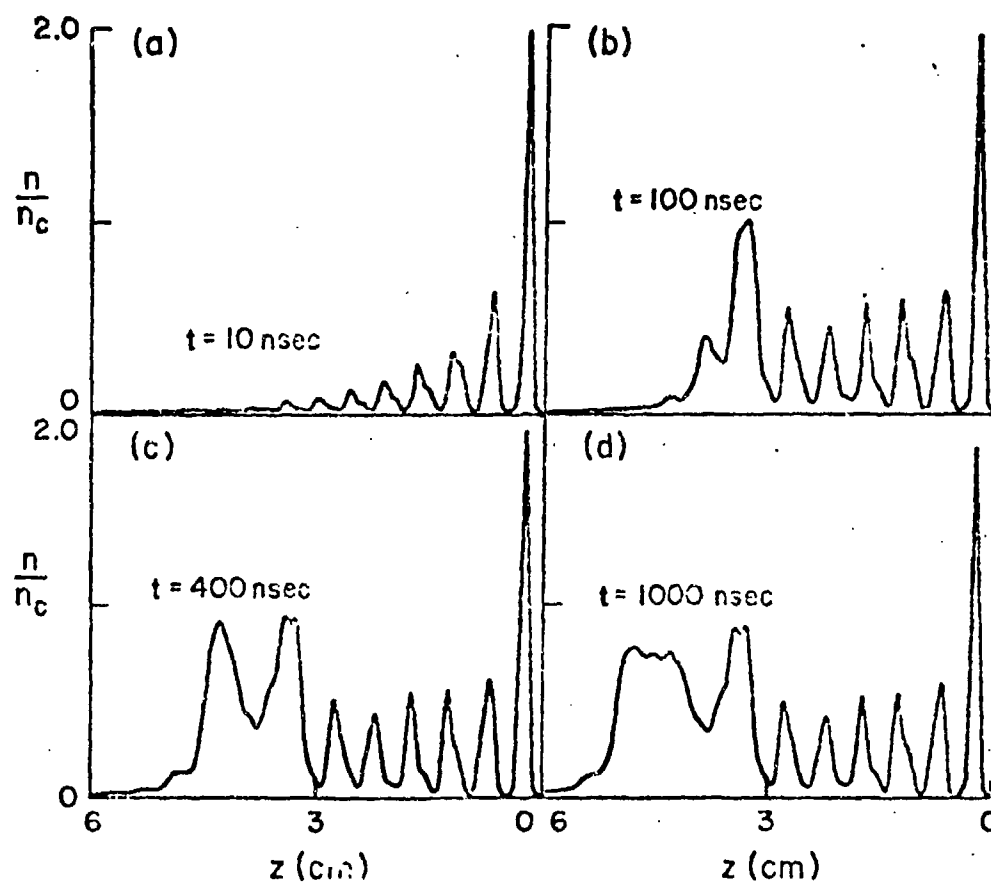


FIGURE 4

Density profiles at 4 different times for the case with a reflector at focus. A spiky structure is observed in this case.

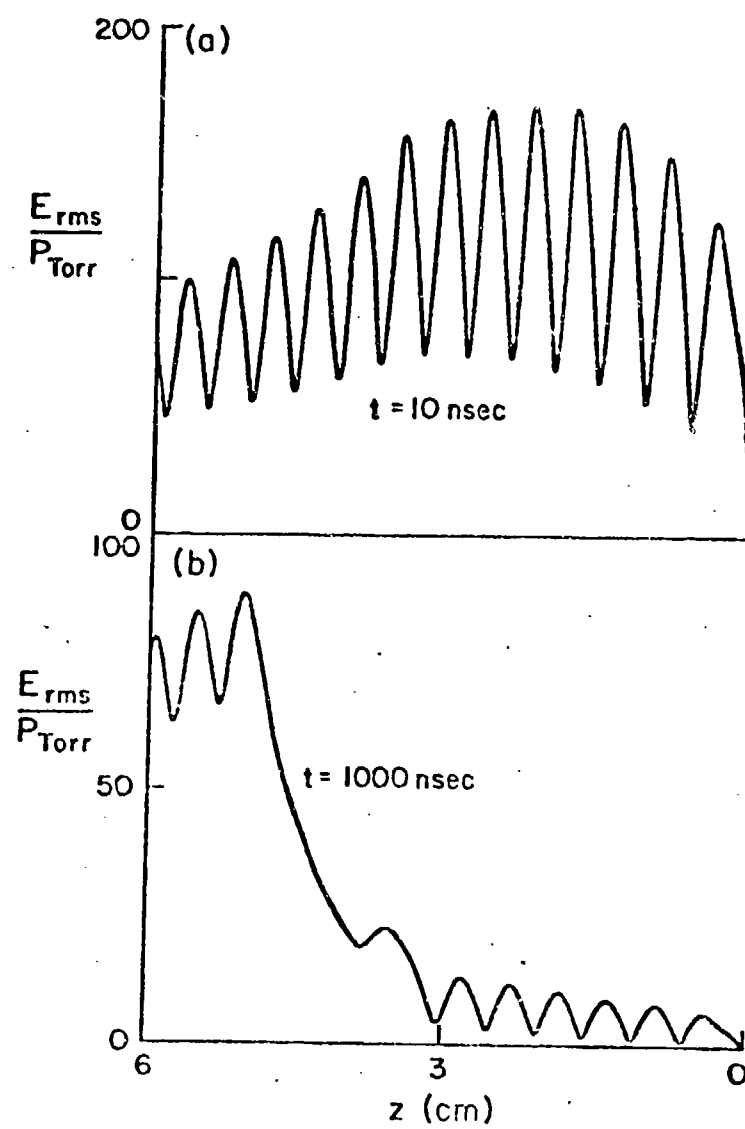


FIGURE 5

Microwave profiles corresponding to the plots in Figure 4.